International Journal of Minerals, Metallurgy and Materials
Volume 19, Number 12, Dec 2012, Page 1149
DOI: 10.1007/s12613-012-0684-1

Fabrication of tungsten films by metallorganic chemical vapor deposition

Yi Li[1,2)], *Jin-pu Li*[1)], *Cheng-chang Jia*[1)], *and Xue-quan Liu*[2)]

1) School of Materials Science and Engineering, University of Science and Technology Beijing, Beijing 100083, China

2) Powder Metallurgy Laboratory, Central Iron & Steel Research Institute, Beijing 100081, China

(Received: 5 March 2012; revised: 10 May 2012; accepted: 11 May 2012)

Abstract: Tungsten films growing on copper substrates were fabricated by metallorganic chemical vapor deposition (MOCVD). The chemical purity, crystallographic phase, cross-sectional texture, and resistivity of the deposited films both before and after annealing treatment were investigated by X-ray energy-dispersive spectroscopy (EDS), X-ray diffraction (XRD), scanning electron microscopy (SEM), and four-point probe method. It is found that the films deposited at 460°C are metastable β-W with (211) orientation and can change into α-W when annealed in high-purity hydrogen atmosphere at high temperature. There are small amounts of C and O in the films, and the W content of the films increases with increasing deposition temperature and also goes up after annealing in high-purity hydrogen atmosphere. The films have columnar microstructures and the texture evolution during their growth on copper substrates can be divided into three stages. The resistivity of the as-deposited films is in the range of 87-104 μΩ·cm, and low resistivity is obtained after annealing in high-purity hydrogen atmosphere.

Keywords: thin films; tungsten; metallorganic chemical vapor deposition; crystallography; textures; electric properties

[*This work was financially supported by the National High-Tech Research and Development Program of China (No.2009AA03Z116).*]

1. Introduction

Refractory metal tungsten possesses many excellent properties, such as high melting point, low vapor pressure, superior abrasive resistance, outstanding anti-corrosive performance, and high electrical conductivity, which make tungsten often used as contact barriers [1-2], low resistance gate materials [3], and metals for interconnections [4]. Tungsten has been widely used in aerospace, electronics, weapons, and chemistry industries.

Many kinds of techniques including low-pressure plasma spraying [5], thermionic vacuum arc method [6], sputtering [7], laser-ablation [8], molten salt electroplating [9], and chemical vapor deposition (CVD) have been employed to fabricate tungsten films. Compared with other techniques, the advantages of CVD processes are extremely attractive because of the low deposition temperature and the controlled morphology and composition of tungsten films by changing deposition conditions.

Different source compounds such as WF_6, WCl_6, and $W(CO)_6$ [10-12] can be used as the source in CVD technology. As a product from hydrogen reduction reaction, hydrogen halide may corrode the reaction chamber with the presence of tungsten halide. Thermal decomposition of $W(CO)_6$ can avoid this problem at a temperature of over 200°C. In this paper, we investigated the preparation of tungsten films using metallorganic chemical vapor deposition (MOCVD) from a precursor of $W(CO)_6$. The properties of tungsten films were determined using X-ray energy-dispersive spectroscopy (EDS), X-ray diffraction (XRD), scanning electron microscopy (SEM), and four-point probe method.

2. Experimental

The source compound $W(CO)_6$ used in this study was independently synthesized by a carbonyl laboratory, and the purity of the solid $W(CO)_6$ precursor reached 99.9%. High-purity (99.99%) hydrogen was used as the carrier gas.

Corresponding author: Jin-pu Li E-mail: lipu716@163.com

The used substrates were pure copper, and the polished substrates were cleaned in acetone using the following procedures: 20-min ultrasonic cleaning to remove extraneous matters on the substrate surface then 2-min de-ionized water rinse.

The MOCVD reactor is shown in Fig. 1. The MOCVD system can be divided into four main components: the gas transport system, the growth system, the temperature control system, and the exhaust gas treatment system. The MOCVD reactor is made of quartz glass. The copper substrate in the reactor was heated with a stainless steel heater. The substrate temperature was measured using a K-type thermocouple and the change of the substrate temperature was controlled by a CKW-1100 automatic temperature indicator-controller. The source compound $W(CO)_6$ was loaded in a evaporator also made of quartz glass, and the sublimation temperature of $W(CO)_6$ was controlled by a HH-SA digital thermostat oil bath pot. The gas transport system controls the amount of source compound $W(CO)_6$ that was supplied to the reaction chamber. Through this gas transport system, a carrier gas of high-purity hydrogen was fed through the evaporator containing the solid source compound $W(CO)_6$, and the flow rate of carrier gas was 200 cm^3/min. The vaporization temperature of $W(CO)_6$ precursor was in the range of 80-105°C. Typically, the tube that transports gaseous $W(CO)_6$ was maintained at 80°C with a heating tape. Tungsten films were deposited over the temperature range of 300-500°C, and the typical film growth periods was 1-5 h. After the deposition, the annealing of the as-deposited films was carried out using a high-temperature tube furnace in high-purity hydrogen atmosphere, the annealing temperature could be changed in the range of 800-900°C and controlled by a K7-A300-PK1011S1A precision temperature controller, and the annealing time was 2 h.

The thickness and texture of tungsten films were examined using a JSM-6510 SEM. A D/max-RB XRD with monochromatic Cu K_α radiation was performed to identify the phases of the films, the composition of the films was measured using EDS, and the sheet resistance of the films was measured using a SB100A/1 four-point probe.

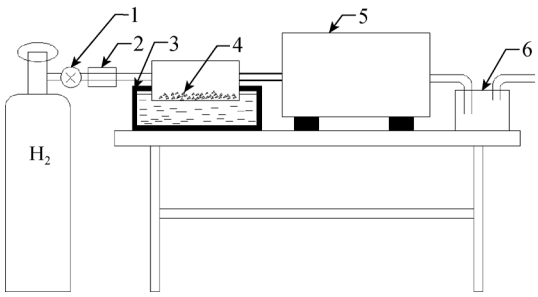

Fig. 1. Schematic illustration of MOCVD for W (1—needle valve; 2—flow meter; 3—oil bath pot; 4—$W(CO)_6$; 5—reactor; 6—exhaust treatment equipment).

3. Results and discussion

3.1. Composition of tungsten films

Tungsten films were deposited at 300, 380, and 460°C, respectively, and the deposition time of the three samples was 5 h. They were then annealed in high-purity hydrogen atmosphere at 900°C for 2 h. EDS spectra of all the thin films are shown in Fig. 2. Fig. 2 illustrates that the films contain C and O besides W. The composition of tungsten films deposited at different temperatures is given in Fig. 3, revealing that the content of W increases with increasing deposition temperature between 300 and 460°C. The W content of the as-deposited films is between 92wt% and 96wt%. The EDS spectrum of the annealed tungsten film deposited at 300°C, depicted in Fig. 2(b), shows that the

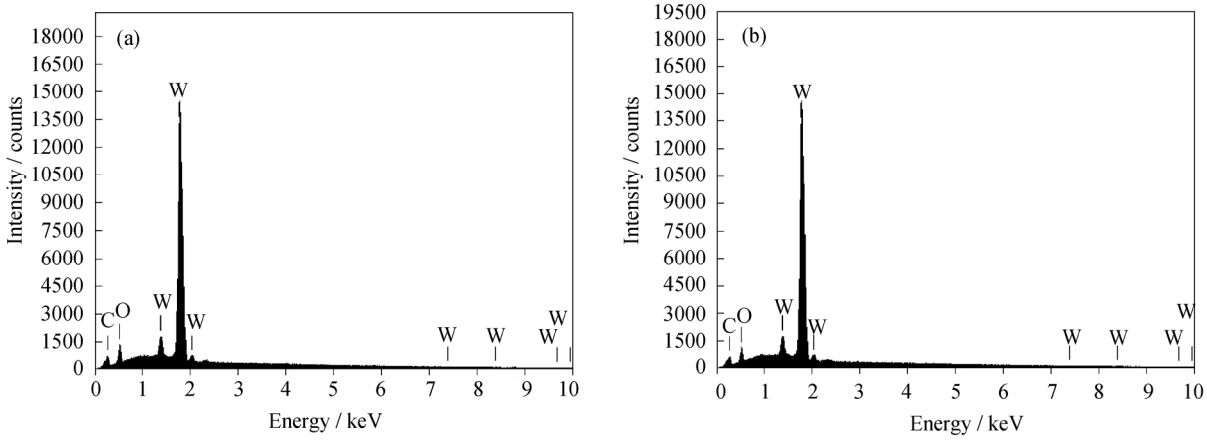

Fig. 2. EDS of tungsten films: (a) film deposited from $W(CO)_6$ at 300°C for 5 h; (b) film deposited from $W(CO)_6$ at 300°C for 5 h and annealed at 900°C for 2 h in high-purity hydrogen atmosphere.

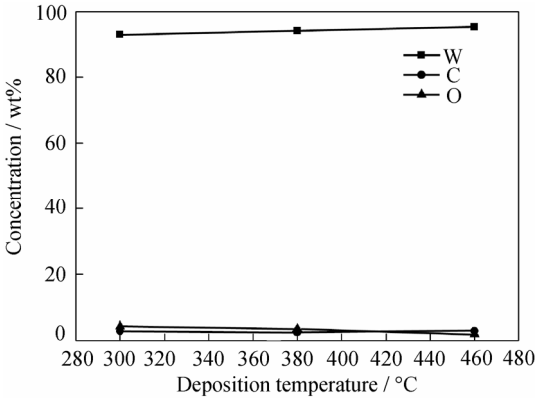

Fig. 3. Effects of deposition temperature on the contents of tungsten, carbon, and oxygen in the deposited films.

film still contains W, C, and O. However, the content of W in the film increases from 92.91wt% to 97.64wt% after annealing at 900°C in high-purity hydrogen atmosphere, and the impurities in the film decrease to a value less than 3wt%.

The source compound $W(CO)_6$ decomposed into W atoms and CO when vaporized and fed into the reactor. At the same time, most of the reaction byproduct CO was excluded from the system, but a small quantity of adsorbed CO decomposed into C and O atoms, which could be combined with W atoms to form tungsten oxide or tungsten carbide as illustrated in Fig. 4. Especially, when the content of CO in the reactor is increased, there are also some carbon and oxygen atoms trapped in the tungsten lattice or in between the grain boundaries [13]. CO dissociation is less favourable with increasing deposition temperature. Therefore, much less impurity atoms are incorporated in tungsten films with increasing deposition temperature.

C and O atoms can recombine to form gaseous CO at high temperature, and oxygen is highly active in hydrogen atmosphere. The above two factors result in decreasing the contents of impurities in the film after annealing in high-purity hydrogen atmosphere at high temperature such as 900°C.

3.2. XRD studies of tungsten films

Tungsten can exist in two crystalline modifications: β-W and α-W. Many studies show that β-W is a metastable form of tungsten [14], in which a little heteroatom impurities are present. β-W can change into α-W with a bcc structure when the temperature of tungsten is higher than 630°C. The XRD pattern of the film deposited at 460°C for 2 h is shown in Fig. 4, revealing that tungsten exists in a form of highly oriented β-W. The peak at 43.54° (2θ) in Fig. 4 corresponds to the β-W (211) plane, and the computed spacing d is 0.2077 nm. According to XRD analysis, the film also contains tungsten oxide phase and tungsten carbide phase, but the contents of tungsten oxide phase and tungsten carbide phase are small from the results of EDS analysis in Figs. 2 and 3.

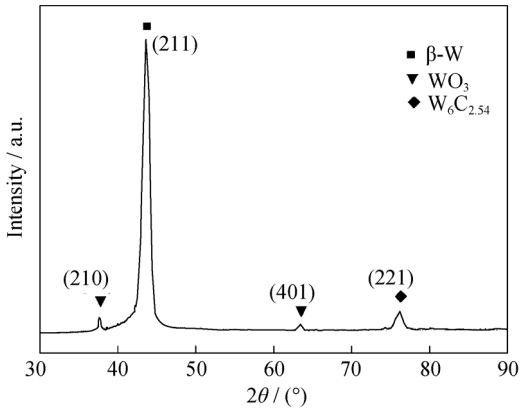

Fig. 4. XRD pattern of the film deposited at 460°C.

The XRD pattern of the deposited film annealed at 800°C in high-purity hydrogen atmosphere, as shown in Fig. 5, indicates the conversion of β-W to α-W. The annealed sample exhibits one sharp tungsten peak, and the sharp peak corresponds to the α-W (110) plane. The annealed tungsten film still contains tungsten carbide phase but not contain tungsten oxide phase.

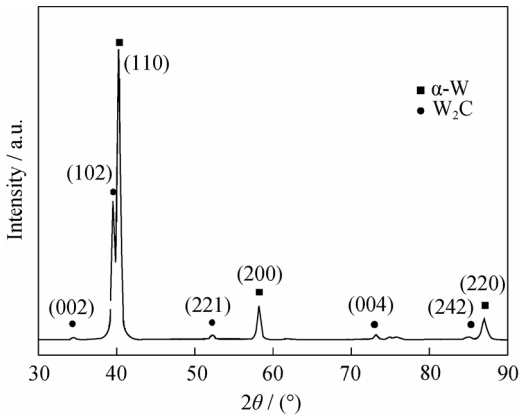

Fig. 5. XRD pattern of the deposited film annealed at 800°C in high-purity hydrogen atmosphere.

Tungsten is partly oxidized on the surface soon after the C–O bond scission takes place. Some C and O atoms are trapped in the tungsten lattice, forming the metastable form of tungsten and a small quantity of tungsten oxide [15]. Annealed around 800°C, C and O atoms recombine as CO, while tungsten is reduced back to its zero valence state and stays into steady state.

3.3. Cross-sectional texture

The microstructural details of tungsten films were ex-

plored from cross-sectional SEM images. Fig. 6 is SEM images obtained from the whole tungsten film thickness.

A 13-μm-thick tungsten film is shown in Fig. 6(a). The SEM images in Fig. 6 provide evidence that the films have columnar microstructures, and a few of small pores are observed in the annealed films. From the SEM images, we can see that the texture evolution during tungsten film growth on copper substrates can be divided into three stages. The film thickness of the initial stage is about 2 μm, and grains formed at this stage are fine because of high nucleation rate and widely spreading growth orientation when the thermal decomposition of $W(CO)_6$ takes place. The film thickness of the second stage is about 1 μm, and crystallites formed at this stage have no orientation. At the third stage, columnar crystals form, and the columnar crystals exhibit strong orientation. From Fig. 6, we can see the formation of uniform, highly oriented columnar microstructures and a few small pores in the annealed films.

3.4. Resistivity of tungsten films

The sheet resistance was measured by four-point probe method, which is usually used to measure the sheet resistance of shallow layers [16]. Tungsten films were deposited by pyrolysis of $W(CO)_6$ at 300, 380, and 460°C in high-purity hydrogen atmosphere, respectively, and the deposition time of the three samples is 5 h. They were then annealed in high-purity hydrogen atmosphere at 800 and 900°C for 2 h. The obtained resistivity values are given in Table 1.

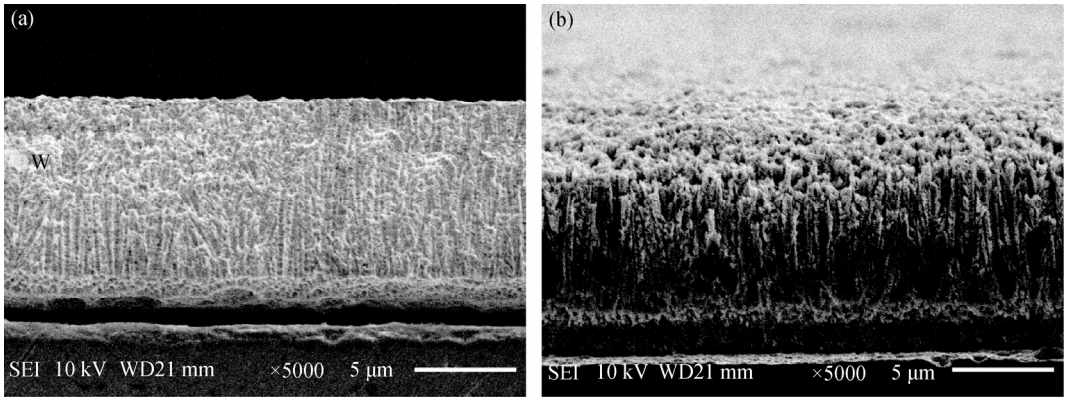

Fig. 6. Cross-sectional SEM images of the W film deposited at 420°C (a) and annealed in high-purity hydrogen atmosphere at 800°C (b).

Table 1. Resistivity of the W films deposited by MOCVD

No.	Deposition temperature / °C	Thickness / μm	Resistivity / (μΩ·cm)	Annealing temperature / °C	Annealing time / h	Resistivity after annealing / (μΩ·cm)
1	300	6.7	104	800	2	41
2	300	6.7	104	900	2	37
3	380	12.5	92	800	2	30
4	380	12.5	92	900	2	28
5	460	11.3	87	800	2	22
6	460	11.3	87	900	2	20

As seen in Table 1, the resistivity values of as-deposited tungsten films with different thicknesses are in the range of 87-104 μΩ·cm, and the resistivity of tungsten films decrease slightly with increasing deposition temperature between 300 and 460°C. For all the samples, the resistivity values decrease after annealing at 800 and 900°C, and their values are in the range of 20-41 μΩ·cm. These phenomena are probably due to the reduction of C and O content between the body and boundaries of grains after annealing.

4. Conclusions

Tungsten thin films were deposited on copper substrates by thermal decomposition of $W(CO)_6$ in high-purity hydrogen atmosphere. The content of W increases with increasing deposition temperature and also increases after annealing in high-purity hydrogen atmosphere. Tungsten films deposited at 460°C are metastable β-W that can change into α-W when annealed in high-purity hydrogen atmosphere at high

temperature. The films have columnar microstructures exhibiting strong orientation, and the texture evolution during tungsten film growth on copper substrates can be divided into three stages. A few of small pores are observed in the annealed films. The resistivity values of as-deposited tungsten films are in the range of 87-104 μΩ·cm. After annealing in high-purity hydrogen atmosphere, the resistivity decreases and their values are in the range of 20-41 μΩ·cm.

References

[1] S. Smith, K. Aouadi, J. Collins, E. van der Vegt, M.T. Basso, M. Juhel, and S. Pokrant, Low resistivity tungsten for contact metallization, *Microelectron. Eng.*, 82(2005), No.3-4, p.261.

[2] H. Körner, E. Bertagnolli, and I. Maier, Contact barrier application of selective CVD-tungsten in a bipolar device, *Appl. Surf. Sci.*, 38(1989), No.1-4, p.497.

[3] S. Schmidbauer, J. Hahn, A. Buerke, F. Jakubowski, O. Storbeck, Y.W. Ting, T. Schuster, and J. Faul, Interface optimization for poly silicon/tungsten gates, *Microelectron. Eng.*, 85(2008), No.10, p.2037.

[4] R. Pantel, H. Wehbe-Alause, S. Jullian, and L.F.T. Kwakman, Analytical transmission electron microscopy observation of aluminium-tungsten interaction in thermally stressed Al/Ti/W/TiN interconnections, *Microelectron. Eng.*, 64(2002), No.1-4, p.91.

[5] Y.R. Niu, X.B. Zheng, H. Ji, L.J. Qi, C.X. Ding, J.L. Chen, and G.N. Luo, Microstructure and thermal property of tungsten coatings prepared by vacuum plasma spraying technology, *Fusion Eng. Des.*, 85(2010), No.7-9, p.1521.

[6] A. Marcu, C.M. Ticoş, C. Grigoriu, I. Jepu, C. Porosnicu, A.M. Lungu, and C.P. Lungu, Simultaneous carbon and tungsten thin film deposition using two thermionic vacuum arcs, *Thin Solid Films*, 519(2011), No.12, p.4074.

[7] G.S. Chen, L.C. Yang, H.S. Tian, and C.S. Hsu, Evaluating substrate bias on the phase-forming behavior of tungsten thin films deposited by diode and ionized magnetron sputtering, *Thin Solid Films*, 484(2005), No.1-2, p.83.

[8] P. Paris, M. Aints, M. Laan, M. Kiisk, J. Likonen, J. Kolehmainen, and S. Tervakangas, Laser ablation of thin tungsten layers deposited on carbon substrate, *Fusion Eng. Des.*, 84(2009), No.7-11, p.1465.

[9] H. Nakajima, T. Nohira, R. Hagiwara, K. Nitta, S. Inazawa, and K. Okada, Electrodeposition of metallic tungsten films in $ZnCl_2$-NaCl-KCl-KF-WO_3 melt at 250ºC, *Electrochim. Acta*, 53(2007), p.24.

[10] K.J. Kuijlaars, C.R. Kleijn, and H.E.A. van den Akker, Modeling of selective tungsten low-pressure chemical vapor deposition, *Thin Solid Films*, 290-291(1996), p.406.

[11] Y. Pauleau, Chemical vapour deposition of tungsten films for metallization of integrated circuits, *Thin Solid Films*, 122(1984), No.3, p.243.

[12] J. Haigh, G. Burkhardt, and K. Blake, Thermal decomposition of tungsten hexacarbonyl in hydrogen, the production of thin tungsten-rich layers, and their modification by plasma treatment, *J. Cryst. Growth*, 155(1995), No.3-4, p.266.

[13] K.A. Gesheva, T.A. Krisov, U.I. Simkov, and G.D. Beshkov, Deposition and study of CVD-tungsten and molybdenum thin films and their impact on microelectronics technology, *Appl. Surf. Sci.*, 73(1993), p.86.

[14] H.M. Huang and X.M. Chen, On the β tungsten to α tungsten transformation, *J. Cent. South Inst. Miner. Metall.*, 18(1987), No.4, p.459.

[15] F. Zaera, Tungsten hexacarbonyl thermal decomposition on Ni(100) surfaces, *J. Phys. Chem.*, 96(1992), p.4609.

[16] M.C. Benjamin, R.J. Hillard, and J.O. Borland, Ultra-shallow junction (USJ) sheet resistance measurements with a non-penetrating four point probe, *Nucl. Instrum. Methods Phys. Res. Sect. B*, 237(2005), p.351.